Advances in Radiation Oncology (2024) 9, 101409

advances in radiation oncology

www.advancesradonc.org

Scientific article

Clinical and Dosimetric Impact of 2D kV Motion Monitoring and Intervention in Liver Stereotactic Body Radiation Therapy

Andrew P. Santoso, PhD,[a,*] Yevgeniy Vinogradskiy, PhD,[b] Tyler P. Robin, MD, PhD,[a] Karyn A. Goodman, MD,[a,c] Tracey E. Schefter, MD,[a] Moyed Miften, PhD,[a] and Bernard L. Jones, PhD[a]

[a]Department of Radiation Oncology, University of Colorado School of Medicine, Aurora, Colorado; [b]Department of Radiation Oncology, Thomas Jefferson University, Philadelphia, Pennsylvania; and [c]Department of Radiation Oncology, Icahn School of Medicine at Mount Sinai, New York, New York

Received 15 June 2023; accepted 13 November 2023

Purpose: Positional errors resulting from motion are a principal challenge across all disease sites in radiation therapy. This is particularly pertinent when treating lesions in the liver with stereotactic body radiation therapy (SBRT). To achieve dose escalation and margin reduction for liver SBRT, kV real-time imaging interventions may serve as a potential solution. In this study, we report results of a retrospective cohort of liver patients treated using real-time 2D kV-image guidance SBRT with emphasis on the impact of (1) clinical workflow, (2) treatment accuracy, and (3) tumor dose.

Methods and Materials: Data from 33 patients treated with 41 courses of liver SBRT were analyzed. During treatment, planar kV images orthogonal to the treatment beam were acquired to determine treatment interventions, namely treatment pauses (ie, adequacy of gating thresholds) or treatment shifts. Patients were shifted if internal markers were >3 mm, corresponding to the PTV margin used, from the expected reference condition. The frequency, duration, and nature of treatment interventions (ie, pause vs shift) were recorded, and the dosimetric impact associated with treatment shifts was estimated using a machine learning dosimetric model.

Results: Of all fractions delivered, 39% required intervention, which took on average 1.9 ± 1.6 minutes and occurred more frequently in treatments lasting longer than 7 minutes. The median realignment shift was 5.7 mm in size, and the effect of these shifts on minimum tumor dose in simulated clinical scenarios ranged from 0% to 50% of prescription dose per fraction.

Conclusion: Real-time kV-based imaging interventions for liver SBRT minimally affect clinical workflow and dosimetrically benefit patients. This potential solution for addressing positional errors from motion addresses concerns about target accuracy and may enable safe dose escalation and margin reduction in the context of liver SBRT.

Sources of support: This work was funded in part by the National Institutes of Health under award numbers K12CA086913 and 5R21CA249647-02, the University of Colorado Cancer Center/ACS IRG #57-001-53 from the American Cancer Society, the Boettcher Foundation, and Varian Medical Systems. These funding sources were not involved in study design; in the collection, analysis, and interpretation of data; in the writing of the manuscript; or in the decision to submit the manuscript for publication.

Data sharing statement: Research data are stored in an institutional repository and will be shared upon request to the corresponding author.

Corresponding author: Andrew Santoso, PhD; E-mail: andrew.santoso@cuanschutz.edu

https://doi.org/10.1016/j.adro.2023.101409

Introduction

Stereotactic Body Radiation Therapy (SBRT) has emerged as an effective, noninvasive treatment option for patients with primary or secondary liver malignancies, and single-institutional trials have reported promising outcomes.[1-7] Local control increases as dose to the tumor is increased,[8,9] but liver SBRT is often hindered by dose to normal liver and other nearby tissues.[10,11] Specifically, respiratory-induced motion of the liver limits the ability to safely deliver high doses per fraction, which in turn leads to reduced local control. Additionally, it has been shown that margins and volumes, such as internal target volumes (ITVs), derived from CT acquisition, can inadequately characterize intrafraction motion in the abdomen.[12-14] By reducing the effect of motion on liver SBRT, it may be possible to increase tumor dose and local control without increasing toxicity.

Real-time, intrafraction tumor position detection is a promising method to account for tumor motion. Fiducial markers are often implanted in or near these tumors to facilitate localization in kV images, and many studies have demonstrated feasibility of using these markers to detect tumor motion in real time.[15-20] However, the effect of interventions based on periodic, intrafraction kV imaging has not been studied. Similarly, implanted electromagnetic transponders have also been used to guide respiratory gating in liver SBRT.[21-23] Most recently, MR imaging has been used during liver SBRT to detect and account for motion,[24] yet the high cost of these complex machines is one reason for limited widespread adoption.

The purpose of this study was to quantify the benefit of kV-based motion monitoring and intervention during liver SBRT treatment. Specifically, the study addresses 3 key questions: What is the effect of intrafraction kV monitoring and correction on (1) clinical workflow, (2) treatment accuracy, and (3) tumor dose?

Methods and materials

Patient population and treatment characteristics

Thirty-three patients with primary liver (eg, hepatocellular carcinoma) or metastatic liver lesions treated with SBRT using a real-time target tracking system were included in this study. Some patients received separate treatments to multiple sites of disease; of these 33 patients, one to 2 courses were identified for a total of 41 SBRT courses for inclusion. Each course consisted of 3 to 5 fractions, cumulating in a total of 171 fractions to be analyzed. Data were collected under an institutional review board-approved protocol for retrospective analysis (COMIRB #17-1004). A summary of demographic information, pertaining to major clinical and treatment characteristics, is provided in Table 1. Internal markers used in conjunction with the real-time tracking system included implanted fiducial markers, the dome of the liver for a single patient for whom anticoagulation could not be safely interrupted, and remnant Lipiodol for patients who had previous procedures. Patients were classified as having 0 fiducials in cases where the liver dome or Lipiodol was used as a marker. For patients with implanted fiducial markers, approximately 1 week before simulation markers were implanted in or near the tumor site by an experienced interventional radiologist. Markers were cylindrical in shape (length, 5 mm; diameter, 0.8 mm) and made of gold (SMG0242-02, Alpha-Omega Services, Inc, Bellflower, CA).

Table 1 Patient demographic information pertaining to the liver SBRT study cohort.*

Characteristics	n (%) or median	Range
All patients	33	-
Number of courses	41	-
Number of fractions	171	-
Compression	8 (24)	-
Gating	25 (76)	-
Dose per fraction, cGy	1000	600-1800
No. of fractions	5	3 or 5
No. of fiducials	2	0-5
Treatment time, s	424	91-1251
PTV volume, cm^3	42	5.4-751

Abbreviations: PTV = planning target volume; SBRT = stereotactic body radiation therapy.
* Note that patients classified as having 0 implanted markers included a single patient whose liver dome was used as a marker and for patients who had remnant lipiodol from previous procedures. All statistics are evaluated on a per course basis

Intrafraction monitoring and motion management strategies

Two motion management strategies were used for both simulation and treatment based on physician preference: compression (10 courses, or 21% of all fractions) or amplitude-based respiratory gating (31 courses, or 79% of all fractions). No patients who underwent 2 treatment courses had differing motion-management strategies. In general, preference was given to gating unless patients had poorly adhered to audio coaching, explained below.[25,26] Abdominal compression was implemented using an indexed, inflatable compression belt (Aktina Medical, Congers, NY). Optimal belt pressure was set by inflating the belt until the patient began to feel pain or discomfort. Abdominal compression patients were simulated

with a free-breathing CT scan under this motion management condition for treatment planning. Gating was accomplished using the Varian Real-time Position Management (RPM) system (Varian Medical Systems, Palo Alto, CA), and treatment was delivered in the end-exhale respiratory phase using amplitude-based gating. For gating patients, an end-exhale breath-hold CT was used for treatment planning. Intravenous (iodine) contrast scans were performed with portal-venous timing to delineate normal liver tissue. Additionally, a 4DCT was acquired to estimate tumor motion. Both breath-hold and 4DCT were acquired in tandem with the RPM system. 4DCT images were sorted retrospectively by phase. Gating patients received audio coaching during the 4DCT, and breathing rate was preselected by the patient. All CT scans were acquired with a 3-mm slice thickness.

Treatment planning

Treatment planning was performed in Eclipse using RapidArc (Varian Medical Systems, Palo Alto, CA). Gross tumor volumes (GTVs) were drawn by the radiation oncologist on the planning CT and expanded to create a planning target volume (PTV). GTV-to-PTV margins were determined on a patient-specific basis, and incorporated information from minimum intensity projection contrast CTs, motion ranges on 4DCT, and local anatomy. GTV-to-PTV expansion margins generally ranged from 3 to 7 mm and were generally largest in the superior-inferior direction. All treatment plans were generated using a 10X-FFF energy at its highest dose rate with 2 to 4 arcs. In patients treated with gating, range of motion was determined from end-exhale phases, defined as the 30% to 70% phases of the 4DCT, which has been demonstrated to have the smallest degree of variability in patients with liver tumors,[27] and was used to create the "fiducial displacement threshold," defined below. For patients treated with compression, the range of motion included all phases. This information is provided for clinical context; however, the GTV-to-PTV margin was not used in our analysis, as the dose model (described below) incorporates a variable margin.

Treatment delivery

Before treatment, patient alignments were evaluated using anterior-posterior (AP) fluoroscopy imaging and cone beam CT (CBCT). Abdominal compression patients were imaged using fluoroscopy to align fiducials to marker contours created during the planning process and then CBCTs were acquired. For patients treated with gating, fluoroscopic imaging was taken during free breathing while receiving the same audio coaching instruction performed at simulation. This verified amplitude gating thresholds set at the time of simulation, as literature indicates 4DCT may underestimate respiratory motion.[12,13,28,29] This was evaluated by determining whether internal markers were within the reference contours. Therapists were instructed to manually stop fluoroscopic image acquisition at end-exhalation and align the captured image to the fiducial contour on the breath-hold simulation CT. Finally, an end-exhale breath-hold CBCT was acquired, and the fiducial markers were used for localization. In cases where patients could not hold their breath for the duration of CBCT acquisition (35 seconds), images were acquired over multiple exhale breath-holds.

Real-time target tracking workflow

Real-time tracking was implemented using the On-Board Imager of a Varian TrueBeam STx system (Varian Medical Systems, Palo Alto, CA). Reference positions were determined that corresponded to the expected location of internal markers. In patients treated with compression, the reference position was the location of the internal markers on the free-breathing planning CT. In patients treated with gating, the reference was the internal marker location on the 30% phase of the 4DCT. This difference results from the real-time kV images being acquired at the beginning of the gating window. A contour expansion margin of 3 mm was added to all reference marker contours to provide a 3-mm tolerance on the expected marker location. In the case of gating, the 3-mm expanded contour encompasses the range of motion of markers over the 30% to 70% phases. This expansion margin is referred to as the "fiducial displacement threshold," as interventions were taken during treatment if the fiducials were observed to have moved outside of this volume.

Intrafraction monitoring

Markers were tracked during treatment using the triggered imaging capabilities of the STx system. During treatment delivery, the system acquired kV planar images orthogonal to the treatment beam and projected the contours of the internal markers onto the acquired images based on the angle of image acquisition. The frequency and timing of image acquisition depended on the motion management strategy used. For abdominal compression, real-time kV images were taken every 20° of volumetric arc therapy delivery. For gating, kV images were acquired at the start of every gated "beam-on" cycle, defined over the 30% to 70% end-exhale phases. In both gating and compression, the time between real-time kV image acquisition was approximately 5-6 seconds. Representative real-time kV images are provided in Figure 1. Therapists were instructed to visually compare the marker locations in acquired images against reference contours. Guidance materials and hands-on training were provided to the

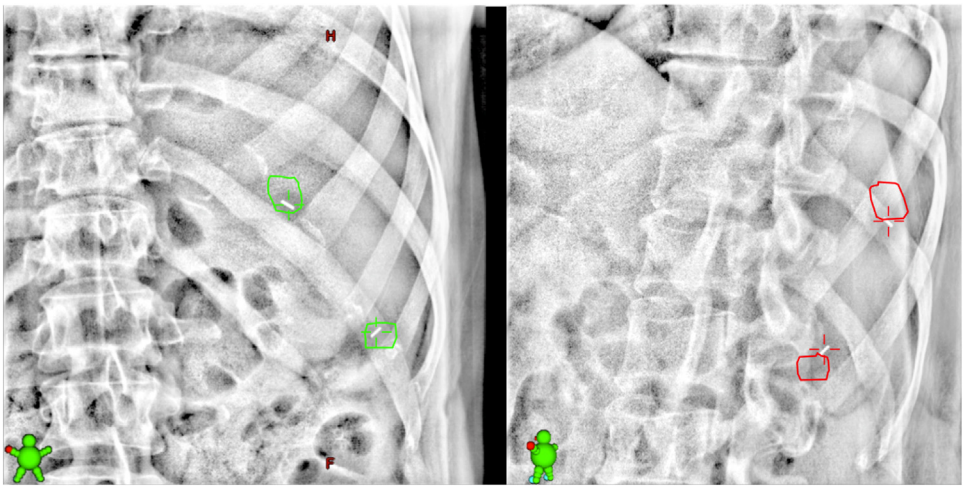

Figure 1 Clinical real-time kV images. Expected fiducial marker locations (plus 3 mm margin) are projected onto kV images acquired during treatment. The image on the left demonstrates markers within the expected area, and treatment proceeded. The image on the right demonstrates markers outside of the expected area, and treatment was halted.

therapists to accomplish this task. If 3 consecutive images demonstrated any of the markers were outside of their contours (ie, motion beyond the fiducial displacement threshold of 3 mm), treatment interventions occurred, described in the following section.

Impact of real-time tracking

Two treatment interventions occurred related to the use of real-time imaging to address errors in treatment delivery. The first intervention is referred to as a *treatment pause,* which involved cases where erratic breathing or baseline drifts would result in gated treatment delivery occurring at the wrong *time.* The effects of erratic breathing and baseline drifts are well documented in the literature and are addressed by this intervention.[25,26] Treatment pauses involved readjusting amplitude gating thresholds without shifting the patient. The second intervention is referred to as a *treatment shift,* which involved cases where patient motion, tumor displacement, or other factors affected tumor position, which would result in treatment delivery occurring at the wrong *place.* Treatment shifts served to relocalize the target and occurred in cases where internal markers were >3 mm from the reference location in 3 consecutive images. The last acquired real-time kV image was used to realign internal markers to the reference location. Note that the system translated 2-dimensional image shifts into a 3-dimensional (3D) couch shift based on the angle at which the real-time kV image was acquired by projecting to isocenter.[30] While it has been demonstrated that real-time kV images can have sub-millimeter agreement with 3D localizing systems, because images were acquired orthogonal to the treatment beam errors in the direction of the treatment beam could not be detected or accounted for until later in the period of gantry rotation.[31] A clinical workflow diagram depicting major processes and decision points is provided in Figure 2.

The impact of this real-time tracking was evaluated by determining the *rate* of the interventions described above. More specifically the *pause* and *shift* rates were defined as the average number of times a pause or shift occurred per fraction, respectively. In the case of treatment shifts, the absolute value of shifts was measured in the AP, superior-inferior (SI), and left-right (LR) directions, and the corresponding *radial* shift, defined as the magnitude of the shift vector, was calculated. These data were extracted from the ARIA oncology information system (Varian Medical Systems, Palo Alto, CA).

All data analysis was performed in MATLAB (MathWorks, Natick, MA). Pause and shift rates were analyzed to evaluate differences in patients attributable to technique, number of fiducials, treatment time, and PTV volume. This was accomplished by performing a multiway analysis of variance to determine significant differences, defined as $P < .05$. Groupings for each independent variable, apart from compression versus gating, were based on the median of the group. To determine the dominant component of the realignment shifts, singular value decomposition (SVD) was performed on the distribution of shifts in this cohort for the SI and AP/LR directions.

Dosimetric analysis of patient alignment

Our previously published artificial neural network-based dosimetric model was used to calculate dosimetric effect of shifts.[32] This model represents a worst-case scenario and is based on prior clinically treated liver SBRT dose distributions, estimating hypothetical 3D dose

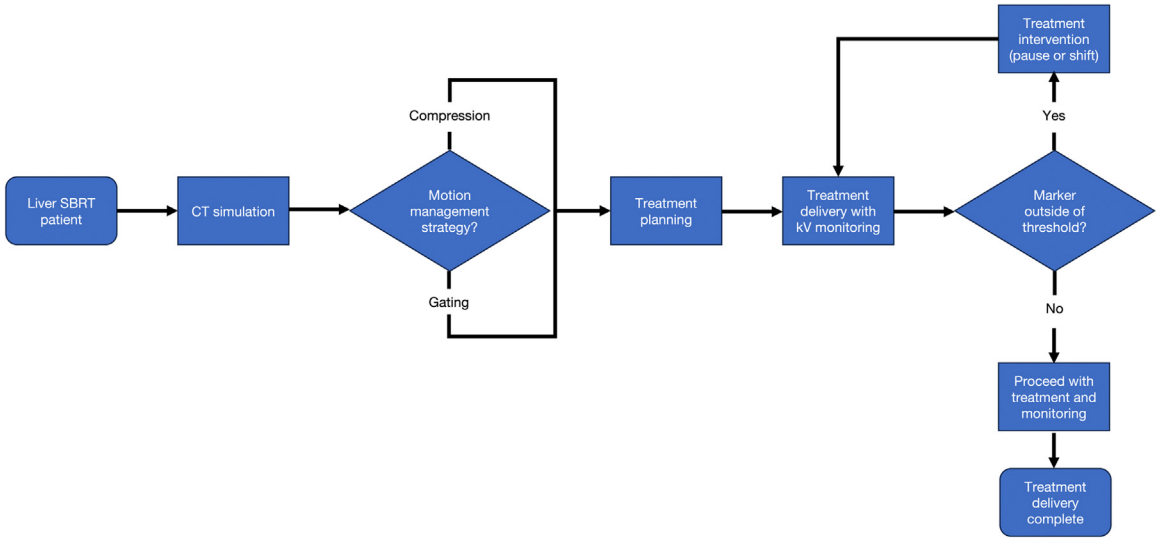

Figure 2 A clinical workflow diagram of real-time 2D kV image tracking for patients treated with liver SBRT. Physician preference determined motion management strategies. Treatment pauses occurred for patients treated with gating due to baseline drift from erratic breathing. Treatment shifts could occur for both motion management strategies when internal markers were outside a 3-mm tolerance of expected location.

distributions based on PTV volume. It models each voxel within 5 cm of the PTV and takes into consideration distance to the PTV, PTV volume, and magnitude of in-plane (SI)/out-of-plane radial shifts to generate a dose-falloff curve that characterizes the 3D dose distribution. By varying the GTV-to-PTV expansion margins, dose-falloff curves were generated in both the SI and radial directions for targets of arbitrary size. Using this, the dosimetric effect of each real-time tracking shift was estimated by calculating dose falloff at that point. This method estimates the minimum point dose to the GTV had it remained at the uncorrected position for the entire duration of treatment. To further understand the dosimetric effect of real-time imaging shifts, point dose difference histograms were generated varying GTV-to-PTV margin expansions from 0 mm to 5 mm.

Results

Data on the pause rate and shift rate, and corresponding statistical analysis, are presented in Table 2. For the entire 41 courses analyzed, the total number of treatment interventions was 118, corresponding to an average intervention rate of 0.69 per fraction. Of the 171 fractions delivered, 39% of fractions had some type of intervention (ie, pause or shift). Treatment pauses (to adjust patient breathing or amplitude thresholds) and shifts (to realign the patient) corresponded to 61% and 39% of treatment interventions, respectively. The average time per intervention was 1.9 ± 1.6 minutes; 9 (8%) treatment interventions were longer than 5 minutes, and one (1%) was longer than 10 minutes. The average time for treatment pauses was 1.6 ± 1.3 minutes, and the average time for shifts was 2.2 ± 1.9 minutes ($P = .054$). The median treatment time, from treatment beam on to beam off, was 7.1 minutes (range, 1.5-20.9 minutes). Both pause and shift rates were significantly higher for patients with longer treatment times ($P < .01$). Figure 3 provides a box plot binning intervention rate (ie, sum of pause and shift rate per patient) according to treatment times: <200 seconds, 200-400 seconds, 400-600 seconds, and >600 seconds. Motion management technique, number of fiducials, and PTV volume were determined not significant for both pause and shift rates ($P > .05$).

Patient realignment triggered by the real-time tracking system occurred 46 times (0.27 shifts per fraction). The distribution of the shifts is shown in Figure 4 as a histogram. The median shifts for patient realignment were 1.4 mm (AP), 4.0 mm (SI), and 1.1 mm (LR). The median radial shift was 5.7 mm. Evaluation of shifts in the in-plane (AP/LR) and SI directions by SVD indicated the dominant shift component was in the SI direction. Of the 171 fractions, 4.7% of SI shifts exceeded 5 mm. Across the 41 courses, 19 (46%) had at least a single 3D shift >5 mm throughout the course of treatment, and 15% of all fractions had at least a single 3D shift that required an alignment >5 mm. No shifts were observed in the compression patient cohort.

Cumulative point dose difference histograms generated from the dosimetric model are shown in Figure 5. For the hypothetical uniform 5-mm PTV margin expansion, 50% of shifts exceeded the size of the margin expansion and resulted in an estimated dosimetric point difference to the GTV. Of these shifts, the average point dose defect was 18 ± 13% of the prescription dose. For margin sizes

Table 2 Statistical analysis of treatment interventions (ie, pauses and/or shifts) occurring during liver SBRT treatment using the real-time tumor tracking system.*

	Treatment pauses		Treatment shifts	
Cohort	**Pause rate (n/fx)**	***P***	**Shift rate (n/fx)**	***P***
All patients (mean)	0.42		0.27	
Technique		**0.57**		**0.91**
Gating	0.40		0.20	
Compression	0.00		0.00	
No. of fiducials		**0.89**		**0.44**
<2	0.33		0.00	
≥2	0.40		0.10	
Treatment time (min)		**<0.01**		**<0.01**
<7.1	0.00		0.00	
≥7.1	0.67		0.33	
PTV volume (cm^3)		**0.10**		**0.40**
<41.9	0.40		0.10	
≥41.9	0.20		0.00	

Abbreviations: fx = fraction; PTV = planning target volume; SBRT = stereotactic body radiation therapy.
* Reported rates are the median of the cohort. Groupings for number of implanted fiducials, treatment time, and PTV volume based on median values of the cohort.

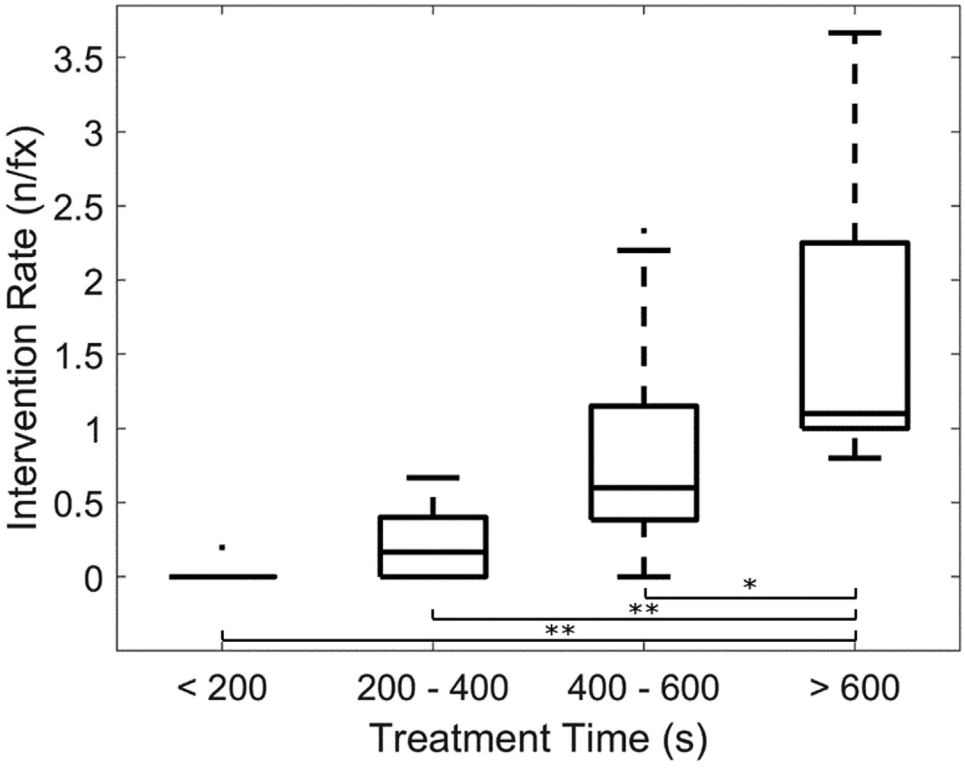

Figure 3 Relationship between the number of treatment pauses and/or shifts per fraction (intervention rate) and treatment time. The intervention rate significantly increases as the treatment time increases. In these box and whisker plots, the inner box shows the 25th to 75th percentile, and the middle line is the median; whiskers represent maxima and minima within 1.5 × interquartile range, and outliers are denoted by black dots; *P* value thresholds of < 0.05 and < 0.001 are denoted by * and **, respectively, and were determined by repeated ANOVA.

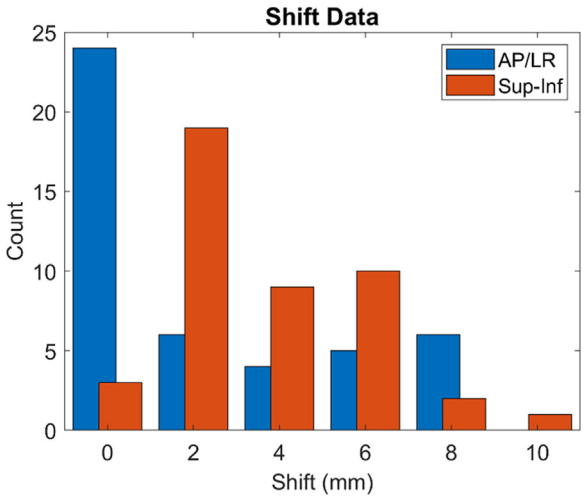

Figure 4 Distribution of shift magnitudes triggered by the real-time tumor tracking system, as provided by the grouped bar chart. Values are shown in the in-plane (AP/LR) and SI directions. The average radial shift was 6.4 mm, and the primary component of these shifts was in the SI direction, as determined by singular value decomposition. *Abbreviations:* AP = anterior-posterior; LR = left-right; SI = superior-inferior.

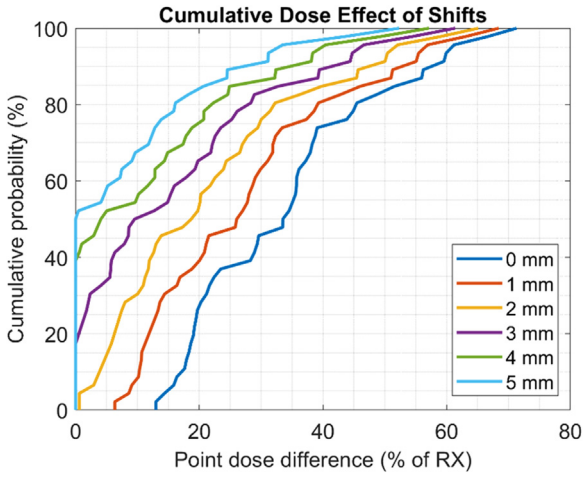

Figure 5 Cumulative point dose difference histograms of variable PTV margin expansion (legend indicating PTV margin expansions of 0 mm to 5 mm) generated using shift data from the liver SBRT cohort and a previously published dosimetric model.[32] For a 5-mm PTV margin expansion, 50% of observed shifts resulted in some kind of dosimetric difference (y-intercept of 50%). In the case of the 0-mm PTV expansion, each shift resulted in a point difference of at least 13% (x-intercept of 13%). *Abbreviations:* PTV = planning target volume; SBRT = stereotactic body radiation therapy.

2 mm or smaller, all shifts had a nonzero estimated point dose difference.

Discussion

Utilization of SBRT in the treatment of liver lesions has continued to grow, requiring careful consideration of confounders, such as motion, that impede ablative radiation doses and dose escalation. In 2010, an ASTRO survey indicated nearly one-third of physicians performed liver SBRT while only 17% of this group were using real-time tumor tracking in this context.[33] In the past decade, the emergence of dedicated real-time tracking systems like MR-guided radiation therapy (MRgRT) have shown promise toward dose escalation through prospective, multi-institutional experiences.[24] Despite these developments, a 2016 ASTRO survey indicated low utilization of MRgRT by sampled physicians (<1%),[34] which may be attributable to the cost of these specialized machines (~$12 million USD per Hehakaya et al[35]) in addition to facility costs. Given the ubiquity of kV-based image guided radiation therapy (IGRT) systems, characterizing clinical and dosimetric impacts kV real-time imaging systems holds promise for addressing dose accuracy concerns due to motion for liver SBRT.

While 4DCT acquired at simulation has proven to be useful in assessing tumor motion, numerous studies have demonstrated this single time point does not capture the range of complex motion on an intrafraction basis.[12,13,28,29] Even widely available IGRT systems like CBCT have been shown to underestimate the ITV, and while 4DCBCT has become more available and can address the variable nature of respiration, it does not directly monitor treatment delivery.[36-39] With these considerations, this work expands limited literature highlighting the effect of real-time kV imaging using a conventional linear accelerator and clinical implementation.

Findings from this study are consistent with existing literature. Results suggest monitoring liver SBRT patients with kV real-time imaging will result in treatment interventions, either readjusting gating thresholds or realigning patients, at a median rate of 0.40 per fraction (mean: 0.69 per fraction, as reported in Table 2). Practically, this suggests interventions will occur 1 in every 3 fractions or 2 in every 5 fractions. The percentage breakdown of treatment interventions of threshold adjustment and patient realignment are consistent with results from real-time imaging for pancreatic SBRT.[25] One major difference is that the intervention rate among liver SBRT patients treated with compression was zero, although it should be noted this study was not powered to quantify the difference in intervention rates between patients treated with gating and compression, and further work on this topic is needed. Our results support that treatment time plays a significant role in terms of treatment intervention rates. Previous reports on abdominal motion indicate deviations from initial setup occur when treatment times exceed 7.5

to 8 minutes, consistent with our results indicating this occurs for liver SBRT when treatment times exceed 7 minutes.[25,40] These data also indicate a potential benefit from treatments that use real-time MLC or couch tracking, as these treatments can achieve a substantially shorter treatment time.[41] Regarding magnitude and frequency of realignment shifts, results from this study complement existing literature by having a larger sample size (n = 33). A 10-patient liver SBRT cohort that used an offline MV-kV imaging technique for intrafraction motion evaluation determined the frequency of SI shifts >5 mm would occur on average 20.3% of the time.[16] An additional retrospective study that evaluated a 19-patient abdominal SBRT cohort using a template-matching algorithm found the frequency of SI displacements >5 mm was 7.6%.[15] This liver SBRT cohort indicated that an online, kV real-time imaging technique results in a lower frequency of shifts, approximately 5% of shifts being of this magnitude.

Primary limitations of this study included the small sample size and the simplicity of the dosimetric model. While treatment pauses were not applicable in the compression patient cohort, the nonsignificant findings of the overall intervention rate are unsurprising given only 8 courses of compression were included in the study. Low intervention rates between gating and compression patients suggest either implementation of motion management will yield a similar clinical burden, but it must be acknowledged that this may be due to the small number of compression data points. Regarding limitations of the dosimetric model, it is a simple point dose model looking at dose-falloff curves generated through machine learning.

Nonetheless, our dosimetric model yielded interesting results and can provide insight on the appropriateness of the size of the fiducial displacement threshold for kV monitoring and intervention. Pertinent follow-up questions are, "Can GTV-to-PTV margins be reduced if intrafraction kV monitoring is used? What is the appropriate size of the fiducial displacement threshold?" Our study used a fiducial displacement threshold of 3 mm, and assuming uniform target margins of 5 mm, 50% of shifts resulted in no dosimetric difference. However, in the hypothetical 2-mm PTV margin expansion scenario, all shifts resulted in a hypothetical dose difference (consistent with previous results for pancreatic SBRT).[25] It is possible that the fiducial displacement threshold or treatment margin expansions may be made smaller when using this real-time imaging intervention approach, but further study is needed. It should be acknowledged that this model represented a worst-case scenario for decreases in PTV coverage attributable to motion estimated over a single fraction without consideration of normal target structures. It also neglects the cumulative dose delivered over all fractions, the portion of dose delivered in error, and additional clinical realities. Despite this model's simplicity, it demonstrated a potential dosimetric benefit and expands the liver SBRT literature for margin reduction or dose escalation. Certainly, further investigation of this kV-based real-time imaging intervention approach and incorporation of additional considerations (eg, fraction of treatment delivered before shifts) is needed to fully characterize dosimetric effect.

Conclusion

In this study, we evaluate the clinical impact of real-time 2D kV imaging on liver SBRT. To date, this data represents the largest experience using real-time kV imaging on a conventional linear accelerator to guide treatment interventions addressing motion. It was determined that after initial alignment with CBCT, patients required interventions for roughly 39% of treated fractions. Use of real-time kV imaging minimally affects clinical workflow, provides a means of addressing intrafraction motion to improve treatment accuracy, and may provide some dosimetric benefit. This data provides insights into the clinical effect of implementing real-time imaging as a tool for liver SBRT treatment interventions.

Disclosures

BLJ and MM report grants from Varian Medical Systems during the conduct of the study, outside of the submitted work. In addition, BLJ and MM have a patent, Automated Tracking of Fiducial Marker Clusters in X-ray Images, US Provisional Patent Application 62/368,870.

References

1. Liu E, Stenmark MH, Schipper MJ, et al. Stereotactic body radiation therapy for primary and metastatic liver tumors. *Transl Oncol*. 2013;6:442-446.
2. Rusthoven KE, Kavanagh BD, Cardenes H, et al. Multi-institutional phase I/II trial of stereotactic body radiation therapy for liver metastases. *J Clin Oncol*. 2009;27:1572-1578.
3. Herfarth KK, Debus J, Lohr F, et al. Stereotactic single-dose radiation therapy of liver tumors: Results of a phase I/II trial. *J Clin Oncol*. 2001;19:164-170.
4. Chang DT, Swaminath A, Kozak M, et al. Stereotactic body radiotherapy for colorectal liver metastases. *Cancer*. 2011;117:4060-4069.
5. Wulf J, Guckenberger M, Haedinger U, et al. Stereotactic radiotherapy of primary liver cancer and hepatic metastases. *Acta Oncol (Madr)*. 2006;45:838-847.
6. Scorsetti M, Arcangeli S, Tozzi A, et al. Is stereotactic body radiation therapy an attractive option for unresectable liver metastases? A preliminary report from a phase 2 trial. *Int J Radiat Oncol Biol Phys*. 2013;86:336-342.
7. Scorsetti M, Clerici E, Comito T. Stereotactic body radiation therapy for liver metastases. *J Gastrointest Oncol*. 2014;5:190-197.
8. Miften M, Vinogradskiy Y, Moiseenko V, et al. Radiation dose-volume effects for liver SBRT. *Int J Radiat Oncol Biol Phys*. 2021;110:196-205.
9. McCammon R, Schefter TE, Gaspar LE, Zaemisch R, Gravdahl D, Kavanagh B. Observation of a dose-control relationship for lung

and liver tumors after stereotactic body radiation therapy. *Int J Radiat Oncol Biol Phys*. 2009;73:112-118.
10. Dawson LA, Normolle D, Balter JM, McGinn CJ, Lawrence TS. Ten Haken RK. Analysis of radiation-induced liver disease using the Lyman NTCP model. *Int J Radiat Oncol Biol Phys*. 2002;53:810-821.
11. Pan CC, Kavanagh BD, Dawson LA, et al. Radiation-associated liver injury. *Int J Radiat Oncol Biol Phys*. 2010;76:S94-S100.
12. Yang W, Fraass BA, Reznik R, et al. Adequacy of inhale/exhale breath-hold CT based ITV margins and image-guided registration for free-breathing pancreas and liver SBRT. *Radiat Oncol*. 2014;9:1-9.
13. Ge J, Santanam L, Noel C, Parikh PJ. Planning 4-dimensional computed tomography (4DCT) cannot adequately represent daily intrafractional motion of abdominal tumors. *Int J Radiat Oncol Biol Phys*. 2013;85:999-1005.
14. Van Den Begin R, Engels B, Gevaert T, et al. Impact of inadequate respiratory motion management in SBRT for oligometastatic colorectal cancer. *Radiother Oncol*. 2014;113:235-239.
15. Yorke E, Xiong Y, Han Q, et al. Kilovoltage imaging of implanted fiducials to monitor intrafraction motion with abdominal compression during stereotactic body radiation therapy for gastrointestinal tumors. *Int J Radiat Oncol Biol Phys*. 2016;95:1042-1049.
16. Worm ES, Høyer M, Fledelius W, Poulsen PR. Three-dimensional, time-resolved, intrafraction motion monitoring throughout stereotactic liver radiation therapy on a conventional linear accelerator. *Int J Radiat Oncol Biol Phys*. 2013;86:190-197.
17. Worm ES, Høyer M, Fledelius W, Nielsen JE, Larsen LP, Poulsen PR. On-line use of three-dimensional marker trajectory estimation from cone-beam computed tomography projections for precise setup in radiotherapy for targets with respiratory motion. *Int J Radiat Oncol Biol Phys*. 2012;83:e145-e151.
18. Li R, Mok E, Chang DT, et al. Intrafraction verification of gated rapidarc by using beam-level kilovoltage X-ray images. *Int J Radiat Oncol Biol Phys*. 2012;83:e709-e715.
19. Poulsen PR, Worm ES, Petersen JBB, Grau C, Fledelius W, Høyer M. Kilovoltage intrafraction motion monitoring and target dose reconstruction for stereotactic volumetric modulated arc therapy of tumors in the liver. *Radiother Oncol*. 2014;111:424-430.
20. Bertholet J, Toftegaard J, Hansen R, et al. Automatic online and real-time tumour motion monitoring during stereotactic liver treatments on a conventional linac by combined optical and sparse monoscopic imaging with kilovoltage x-rays (COSMIK). *Phys Med Biol*. 2018;63:055012.
21. Poulsen PR, Worm ES, Hansen R, Larsen LP, Grau C, Høyer M. Respiratory gating based on internal electromagnetic motion monitoring during stereotactic liver radiation therapy: First results. *Acta Oncol (Madr)*. 2015;54:1445-1452.
22. James J, Cetnar A, Dunlap NE, et al. Technical note: Validation and implementation of a wireless transponder tracking system for gated stereotactic ablative radiotherapy of the liver. *Med Phys*. 2016;43:2794-2801.
23. Worm ES, Høyer M, Hansen R, et al. A prospective cohort study of gated stereotactic liver radiation therapy using continuous internal electromagnetic motion monitoring. *Int J Radiat Oncol Biol Phys*. 2018;101:366-375.
24. Rosenberg SA, Henke LE, Shaverdian N, et al. A multi-institutional experience of MR-guided liver stereotactic body radiation therapy. *Adv Radiat Oncol*. 2019;4:142-149.
25. Vinogradskiy Y, Goodman KA, Schefter T, Miften M, Jones BL. The clinical and dosimetric impact of real-time target tracking in pancreatic SBRT. *Int J Radiat Oncol Biol Phys*. 2019;103:268-275.
26. Mageras GS, Yorke E. Deep inspiration breath hold and respiratory gating strategies for reducing organ motion in radiation treatment. *Semin Radiat Oncol*. 2004;14:65-75.
27. Oh SA, Yea JW, Kim SK, Park JW. Optimal gating window for respiratory-gated radiotherapy with real-time position management and respiration guiding system for liver cancer treatment. *Sci Rep*. 2019;9:1-6.
28. Shirato H, Seppenwoolde Y, Kitamura K, Onimura R, Shimizu S. Intrafractional tumor motion: Lung and liver. *Semin Radiat Oncol*. 2004;14:10-18.
29. Ozhasoglu C, Murphy MJ. Issues in respiratory motion compensation during external-beam radiotherapy. *Int J Radiat Oncol Biol Phys*. 2002;52:1389-1399.
30. Varian Medical Systems. TrueBeam 2.7 MR3 instructions for use. Accessed October 5, 2023. http://www.varian.com/us/corporate/legal/reach.html.
31. Cetnar A, Ayan AS, Graeper G, et al. Prospective dual-surrogate validation study of periodic imaging during treatment for accurately monitoring intrafraction motion of prostate cancer patients. *Radiother Oncol*. 2021;157:40-46.
32. Campbell WG, Miften M, Olsen L, et al. Neural network dose models for knowledge-based planning in pancreatic SBRT. *Med Phys*. 2017;44:6148-6158.
33. Pan H, Simpson DR, Mell LK, Mundt AJ, Lawson JD. A survey of stereotactic body radiotherapy use in the United States. *Cancer*. 2011;117:4566-4572.
34. Nabavizadeh N, Elliott DA, Chen Y, et al. Image guided radiation therapy (IGRT) practice patterns and IGRT's impact on workflow and treatment planning: Results from a national survey of American society for radiation oncology members. *Int J Radiat Oncol Biol Phys*. 2016;94:850-857.
35. Hehakaya C, Van der Voort van Zyp JR, Lagendijk JJW, Grobbee DE, Verkooijen HM, Moors EHM. Problems and promises of introducing the magnetic resonance imaging linear accelerator into routine care: The case of prostate cancer. *Front Oncol*. 2020;10:1-11.
36. Vergalasova I, Maurer J, Yin FF. Potential underestimation of the internal target volume (ITV) from free-breathing CBCT. *Med Phys*. 2011;38:4689-4699.
37. Lee S, Yan G, Lu B, Kahler D, Li JG, Sanjiv SS. Impact of scanning parameters and breathing patterns on image quality and accuracy of tumor motion reconstruction in 4D CBCT: A phantom study. *J Appl Clin Med Phys*. 2015;16:195-212.
38. Ahmad M, Balter P, Pan T. Four-dimensional volume-of-interest reconstruction for cone-beam computed tomography-guided radiation therapy. *Med Phys*. 2011;38:5646-5656.
39. Santoso AP, Song KH, Qin Y, et al. Evaluation of gantry speed on image quality and imaging dose for 4D cone-beam CT acquisition. *Radiat Oncol*. 2016;11:98.
40. Rankine L, Wan H, Parikh P, et al. Cone-beam computed tomography internal motion tracking should be used to validate 4-dimensional computed tomography for abdominal radiation therapy patients. *Int J Radiat Oncol Biol Phys*. 2016;95:818-826.
41. Booth JT, Caillet V, Hardcastle N, et al. The first patient treatment of electromagnetic-guided real time adaptive radiotherapy using MLC tracking for lung SABR. *Radiother Oncol*. 2016;121:19-25.